Chemical Engineering Journal 159 (2010) 220–229

Contents lists available at ScienceDirect

Chemical Engineering Journal

journal homepage: www.elsevier.com/locate/cej

Microparticle formation of sodium cellulose sulfate using supercritical fluid assisted atomization introduced by hydrodynamic cavitation mixer

Qi Wang, Yi-Xin Guan, Shan-Jing Yao*, Zi-Qiang Zhu

Department of Chemical and Biological Engineering, Zhejiang University, Hangzhou 310027, Zhejiang, China

ARTICLE INFO

Article history:
Received 30 September 2009
Received in revised form 26 January 2010
Accepted 1 February 2010

Keywords:
Supercritical fluid assisted atomization
Hydrodynamic cavitation mixer
Sodium cellulose sulfate
Micronization

ABSTRACT

A novel micronization technique so-called supercritical fluid assisted atomization introduced by hydrodynamic cavitation mixer (SAA-HCM) was used to produce the sodium cellulose sulfate (NaCS) microparticles with well-defined spherical morphologies and controlled particle size distributions in aqueous solution. The process parameters such as mixer temperature and pressure, the mass flow ratio, precipitator temperature, solution concentration and the molecular weight of NaCS were investigated in detail to evaluate their influences on the morphologies and size distributions of precipitates. Spherical NaCS particles with mean diameters ranging from 0.3 to 3.0 μm were produced at the optimum operating conditions and narrow particle size distributions were obtained. It is natural to put forward the particle formation mechanism of deflated balloons. Compared with the unprocessed NaCS, there was no significant change on the primary structure and stability of the NaCS processed by SAA-HCM verified by Fourier transform infrared spectroscopy. The X-ray diffraction and thermo-gravimetric analysis were also used to investigate NaCS modifications and a slight change in crystalline state with higher thermal stability was observed when treated by SAA-HCM process. The results indicated that NaCS micronization by SAA-HCM process was expected to be a promising technique for drug delivery system.

1. Introduction

Microparticle drug delivery system such as inhaled aerosols is an effective therapeutic carrier for the treatment of respiratory inflammation, cystic fibrosis, and other lung disorders; it also offers great potential for noninvasive systemic delivery of peptides and proteins with no gastrointestinal tract degradation [1]. Local or systemic inhalation therapies can often benefit from a controlled release of the therapeutic agent, as is achievable with the use of biodegradable and biocompatible polymeric materials [2,3]. Sustained controlled release from the inhaled therapeutic microparticles can prolong the efficacy of an administered drug and can diminish the rate of a drug's appearance in the bloodstream [3]. Also, patients will experience significantly less pain when dosage frequency is reduced. Among these various formulations, hydrophilic matrix microparticles with smooth surface and narrow size distributions are considered to be one of the most significant release systems to be used as carriers for drug delivery and cell attachment [4,5]. One favorable characteristic of hydrophilic polymer is its water-solubility and potential pharmaceutical application since solvent residues in the micronized particles could be avoided by using water instead of organic solvents. This biocompatible system with suitable forms and size distributions can be applied in various advanced drug delivery strategies due to the enhancement of the bioavailability of biological active substance.

Nowadays, there are still several difficulties in the micronization of hydrophilic polymers, such as the inactivation of the monomer residues during polymerization, high disposal temperature, limited size control, and the difficulty to reduce the solvent residues below the FDA limits in further operation. To solve these problems, a promising alternative process of supercritical fluid (SCF) based technology has turned into researchers' attention. It takes advantage of some specific properties of SCF such as the large diffusivity, strong solvent power, low viscosity, surface tension and environment benign. However, it is still a blank on hydrophilic polymer microparticles production using SCF-based processes in aqueous solution. It was well known that the solubility of water-soluble polymer in SC-CO_2 is nearly zero and SC-CO_2 is not an effective solvent for aqueous solutions, so conventional SCF-based micronization technologies had some difficulties in preparation of microparticles of water-soluble polymers. These conventional techniques included the rapid expansion of supercritical solutions (RESS) [6], the supercritical antisolvent precipitation (SAS) [7], and the particles from gas saturated solution (PGSS) [8]. Recently the supercritical assisted atomization (SAA) which was developed firstly by Reverchon et al. [9–11], was proposed as one of the most potential efficient micronization technique. It could be

* Corresponding author. Tel.: +86 571 87951982; fax: +86 571 87951982.
E-mail address: yaosj@zju.edu.cn (S.-J. Yao).

1385-8947/$ – see front matter © 2010 Elsevier B.V. All rights reserved.
doi:10.1016/j.cej.2010.02.004

considered as a modification of the spray drying with moderate ambient and well size control of the water-soluble material in the aqueous solution. This process has been successfully applied in the preparation of chitosan [12], hydroxypropyl methylcellulose (HPMC) [13] microparticles, chitosan–ampicillin trihydrate [14] and HPMC–ampicillin trihydrate coprecipitates [13] to obtain controlled release of the ampicillin trihydrate. However, there were several concavities presented in the HPMC powder, meanwhile, no further analysis and optimization on particle morphologies and size distribution were present in their research.

One of the most crucial prerequisites for a successful SAA precipitation of hydrophilic polymers was the complete mixing between CO_2 and aqueous solution [15,16]. Based on the solubilization of controlled quantities of SC-CO_2 in aqueous solution, a near-equilibrium solution formed in the mixer was subsequently atomized through a nozzle. The spatial homogeneity of atomized droplets means the uniformity degree of the precipitated particles which depends on the efficiency of the mass transfer between SC-CO_2 and aqueous solution. When using water as a solvent, the solubilization of controlled quantities of SC-CO_2 in aqueous solution is quite limited. Thus, forming a "homogeneous" mixing is even more important in order to obtain a continuous near-thermodynamic-equilibrium solubilization of SC-CO_2 in the liquid solution. Besides, failed primary atomization, which was usually caused by the high viscosity and the surface tension of the aqueous solution, was not negligible [12].

In 2008, Cai et al. [17] implemented an improved SAA process, i.e. SAA-HCM, in which a hydrodynamic cavitation mixer was introduced to intensify the mixing between CO_2 and liquid feedstock. In the mixer, an orifice plate was designed as the cavitation generator. When the resulting premixed fluid flowed through the orifice plate, the amount of the CO_2 mixed with the aqueous solution transited into the transient bubbles driven by pressure variation. Thus, the liquid region generated a number of CO_2 cavities, which subsequently collapsed owing to the recovery of the pressure after the orifice. The implosions of these cavities along with the transient high energy can disrupt the phase boundary [18], increase the interfacial area [19] and create microjets. The generation of the cavities, i.e. hydrodynamic cavitation, was a useful tool for strengthening mass transfer of heterogeneous system [18]. This was one of the most significant steps in the SAA-HCM process. Since the efficiency of the following atomization in the interior of the primary droplets depended upon the CO_2 content, the homogeneous mixture induced smaller particles. SAA-HCM had been applied successfully in the micronization of levofloxacin hydrochloride [17] with well-defined spherical morphology and controlled particle size distribution (PSD). The perfect mixing of the ternary mixture in the hydrodynamic cavitation mixer can reduce the viscosity and the surface tension of the aqueous solution efficiently [20], increase the homogeneity of the primary droplets and could provide a better particle morphology and size distribution control in the production of microparticles.

Sodium cellulose sulfate (NaCS) was a kind of the hydrophilic derivatives of cellulose, which was obtained by a heterogeneous sulfating process with *n*-propanol and H_2SO_4 [21,22]. Due to its favorable biological properties, including nontoxicity, biocompatibility, biodegradation, hydrophilicity, and good film-forming performance [4,21–25], NaCS has been received much attention and widely used in many fields, especially in pharmaceutical and biomedical engineering. In particular, NaCS was frequently used as a polyanion encapsulation matrix to immobilize enzymes, microorganisms and animal/plant cells or as a swellable hydrophilic matrix applied in the drug delivery system which forms a gel layer when exposed to aqueous media.

In the present study, the micronization of NaCS polymer with a controlled size, suitable for drug delivery system using the SAA-HCM process was investigated. The produced NaCS microparticles, using water as solvent, were characterized according to their morphologies and particle size distributions. The influences of process parameters on morphologies and size distributions of precipitated microparticles were evaluated as well. The main structure, the crystalline state and the thermal property of the samples after the SAA-HCM treatment were analyzed with FTIR, XRD and TGA, respectively.

2. Experimental

2.1. Materials

Sodium cellulose sulfate (NaCS, *Mw* = 633 kDa, 120 kDa, 5 kDa) with different molecular weights were prepared by heterogeneous reaction as described previously in our research [4]. Carbon dioxide (CO_2, purity 99%) and nitrogen (N_2, purity 99%) were purchased from Hangzhou Jingong Gas Co. Ltd. (Hangzhou, China). Ethanol (analytical purity) was obtained from Hangzhou Chemical Reagent Co. Ltd. (Hangzhou, China). Deionized water was prepared in our laboratory. All other chemicals used were of analytical grade without any further purification.

2.2. The SAA-HCM apparatus

Fig. 1 presents a schematic diagram of the SAA-HCM apparatus employed for sodium cellulose sulfate precipitation, which consists of three feed lines for delivering the liquid carbon dioxide, the aqueous solution and the inert gas nitrogen, with three main vessels of the hydrodynamic cavitation mixer, the precipitator and the separator. The detailed description of this experimental apparatus and its operating procedure has been given elsewhere [17]. In the beginning, carbon dioxide, stored in a cylinder container, was cooled in the cooling bath (Re) and delivered into the high-pressure pump (P_1) to maintain a constant feeding rate. Then the carbon dioxide went into the mixer (Mi) after being heated up to the desired temperature in the water bath (H_3). Meanwhile, the prepared solution was pumped by high-pressure pump (P_2) with its feeding temperature controlled by a heat exchanger (H_1). The carbon dioxide and the liquid solution were mixed in the hydrodynamic cavitation mixer (Mi) to form the polymer–solvent–CO_2 ternary mixture with a constant temperature and pressure. The mixture was sprayed into the precipitator (Pr, 35L) through a thin-walled 200 μm diameters stainless steel injection nozzle. To facilitate liquid droplets evaporation, a controlled flow of N_2 was heated in an electric heat exchanger (H_2) and then sent to the precipitator. The dry particles were collected in a 0.5 μm pore size stainless steel filter at the bottom of the drying chamber. The gas mixture of CO_2, N_2 and water vapor permeated through the filter and entered the separator (Sp) where the liquid solvent was collected. The maximum pressure error was about ±0.1 MPa, and the maximum temperature error was about ±1 °C.

2.3. Process conditions

A multilevel single-factorial 1^6 experimental design was performed to investigate the influence of the mixer temperature (*Tm*), the mixer pressure (*P*), the mass flow ratio (*R*), the precipitator temperature (*Tp*), the initial solute concentration (*C*), and the molecular weight of the NaCS (*Mw*) on the morphologies and the size distributions of the precipitates. The range of the investigated process parameters was selected base upon the literature [12–17] and the binary phase equilibrium of the solvent and CO_2. The operating parameters are summarized in Table 1. About 1.5 g of powder was produced with 90% of the yield in each run (calculated as the ratio of the powder collected and the solutes fed to the apparatus). All

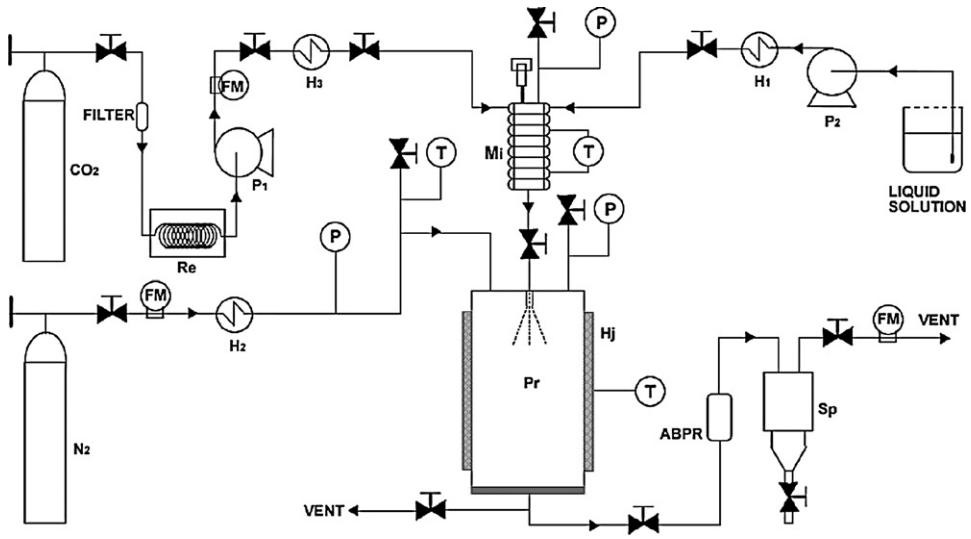

Fig. 1. Schematic representation of SAA-HCM. H_1, liquid solution heat exchanger; H_2, nitrogen heater; H_3, carbon dioxide heater; Re, cooling bath; P_1 and P_2, high-pressure pumps; Mi, mixer; Pr, precipitator; ABPR, automatic back pressure regulator; Sp, separator; Hj, heating jackets; P, pressure indicator; T, temperature indicator; FM, mass flow meter.

measurements were carried out in triplicate, and the averages were adopted in the data analysis.

2.4. Particle characterization

The morphologies of particulate samples were characterized with field emission scanning electron microscope (SEM, JSM-6390A, JEOL, Japan). Particle size analysis was performed by particle image analysis software (Image-Pro Plus 5.0, Media Cybernetics Inc., USA) and about 1000 target particles were considered in each particle size distribution calculation. The particle size distribution was analyzed by Microcal Origin Software (release 7.5, Microcal Software Inc., Northampton, USA) and then converted into number distribution by the Systat Software (TableCurve 2D 5.01, Systat Software Inc., USA). At least 10 SEM images were taken at different locations in the precipitator in each run to verify the uniformity.

A Fourier transform infrared spectrometer (FTIR, Nicolet 5700, USA) was used to characterize the original NaCS polymer and microparticles prepared by the SAA-HCM process. The particles were ground with KBr powder and then pressed to films of 0.2 mm thickness. FTIR spectra were recorded on those films over the wavenumber range of 4000–400 cm^{-1} at ambient temperature with a resolution of 4 cm^{-1}.

The thermal properties of the NaCS microparticles were investigated by the thermo-gravimetric analysis (TGA, Perkin-Elmer

Table 1
Process parameters of SAA-HCM experiments performed on NaCS.

Run	C/mg ml^{-1}	R	Tm/°C	P/MPa	Tp/°C	Mw/kDa	Solvent
Effect of the mixer temperature, Tm							
1	2.4	2.0	60	9.0	100	633	Water
2	2.4	2.0	70	9.0	100	633	Water
3	2.4	2.0	80	9.0	100	633	Water
Effect of the mixer pressure, P							
4	5.0	2.0	70	8.0	100	633	Water
5	5.0	2.0	70	10.0	100	633	Water
6	5.0	2.0	70	11.5	100	633	Water
Effect of the mass flow ratio, R							
7	2.4	2.0	70	9.0	100	633	Water
8	2.4	1.5	70	9.0	100	633	Water
9	2.4	0.7	70	9.0	100	633	Water
Effect of the precipitator temperature, Tp							
10	1.0	2.0	70	9.0	80	633	Water
11	1.0	2.0	70	9.0	120	633	Water
12	12.0	2.0	70	10.0	100	633	Water + ethanol
Effect of the solute concentration, C							
13	1.0	2.0	70	10.0	100	633	Water
14	2.0	2.0	70	10.0	100	633	Water
15	5.0	2.0	70	10.0	100	633	Water
16	12.0	2.0	70	10.0	100	633	Water
Effect of the molecular weight, Mw							
17	2.4	2.0	70	9.0	100	633	Water
18	2.4	2.0	70	9.0	100	120	Water
19	2.4	2.0	70	9.0	100	5	Water

Pyris-1, USA). A small amount of samples were heated from 30 to 800 °C under nitrogen atmosphere at a heating rate of 10 °C min^{-1}.

Diffraction patterns of precipitated NaCS powders were obtained using an X-ray diffractometer (X'Pert PRD, PANalytical, Holland). The measuring conditions were as follows: Ni-filtered Cu Kα radiation, target at 40 kV and 40 mA, 2θ angle ranging between 10° and 80° with a scan rate of 10 s/step and a step size of 0.0167°.

3. Results and discussion

In general, the solubilization of SC-CO_2 in the aqueous solution inside the mixer was a key step for controlling the efficiency of the standard SAA technology [12–16]. The solubilization depends on the temperature *Tm*, the pressure *P* in the mixer and the mass flow ratio *R* between the CO_2 and aqueous solution, because it is related to high-pressure vapor–liquid equilibrium (VLE) of the selected ternary polymer–water–CO_2 mixture. It was not available in this case to obtain the VLE data that the presence of the solute can modify the VLE. Hence, only semi-empirical study of the effect of this parameter should be necessary. The data of vapor–liquid phase boundaries were available in the literature [26] for binary system containing water and CO_2 at the temperatures from 323 to 353 K over a wide range of pressures (0–16 MPa). In addition, the suitable precipitator conditions can make sure the complete evaporation of the solvent and minimize the thermal stress on the treated compound. The physicochemical properties such as the concentration *C* of the solute and molecular weight *Mw* should be regarded as important factors for the particle morphologies and the size distributions. The detailed experimental results are discussed as follows.

3.1. Effect of the mixer temperature

The influences of the mixer temperature *Tm* on the morphology and the size distribution of the precipitated particles were investigated and Fig. 2 shows the SEM micrographs of runs 1–3, at different mixer temperature. The particle size distributions in terms of particle number of the NaCS microparticles prepared at different temperature in the mixer are given in Fig. 3. Compared with the unprocessed amorphous original NaCS material with the block of irregular shape and the size of several hundreds micrometers, the NaCS microparticles were prepared successfully by the SAA-HCM with well-defined spherical morphology, smooth surface and narrow distribution between 0.3 and 4.0 μm. Besides, it is obvious that the mixing temperature had almost no effect on the morphology of the particles, which presented the well-defined spherical smooth surface. There was only a slight shift of the particle size distribution towards narrow region with the increase of the mixer temperature.

The influence of the mixer temperature *Tm* on the particle size lies in two aspects [15,16]: the one is that the viscosity and the surface tension of the aqueous solution decreases with the mixer temperature increase; the other is that the increase of mixer temperature can reduce the quantities of the CO_2 dissolved in the liquid solution. The two opposite effects counteract each other. However, since water is usually more viscous than organic liquid as a solvent, especially for the high-molecular-weight polymer solution, the solubility of the CO_2 in the aqueous solution changes very little ($\Delta X_{CO_2} < 0.01$) according to the vapor–liquid equilibrium of CO_2–water system. Consequently, a slight change of the particle size distribution occurred accordingly in the different mixer temperature at low solution concentration. Moreover, when NaCS was applied in the pharmaceutical and food fields, 70 °C was chosen as the suitable mixer temperature.

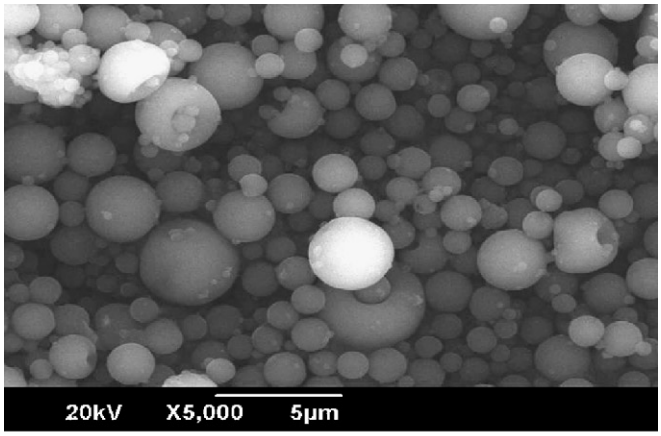

(a) ×5000

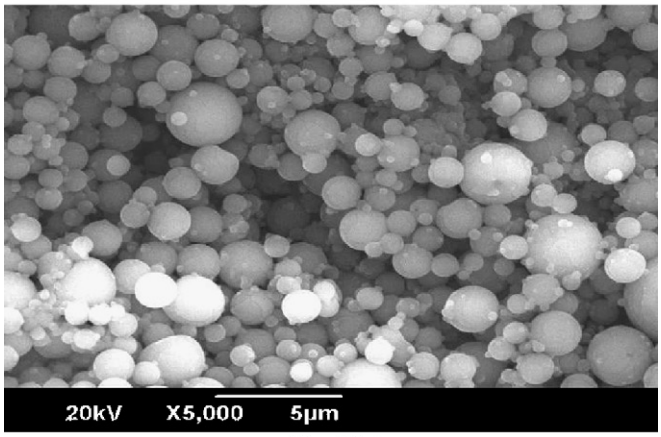

(b) ×5000

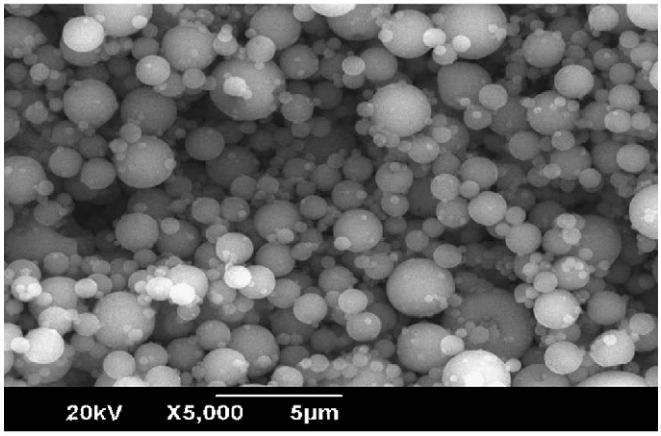

(c) ×5000

Fig. 2. SEM micrographs of NaCS precipitated by SAA-HCM from runs 1 to 3 with different mixer temperature, at (a) *Tm* = 60 °C, (b) *Tm* = 70 °C, and (c) *Tm* = 80 °C, at *P* = 9.0 MPa, *R* = 2.0, *Tp* = 100 °C, *C* = 2.4 mg ml^{-1}, and *Mw* = 633 kDa.

3.2. Effect of the mixer pressure

The influence of the mixer pressure *P* on the morphology and the size distribution of resulting particles were studied in a range of 8.0–11.5 MPa. The particle size distributions in terms of particle number at the different mixer pressures are shown in Fig. 4. The influence of mixer pressure on the morphology and size distribution of the precipitates was more sensitive than that of the mixer temperature.For example, at the mixer pressure of 8.0 MPa,

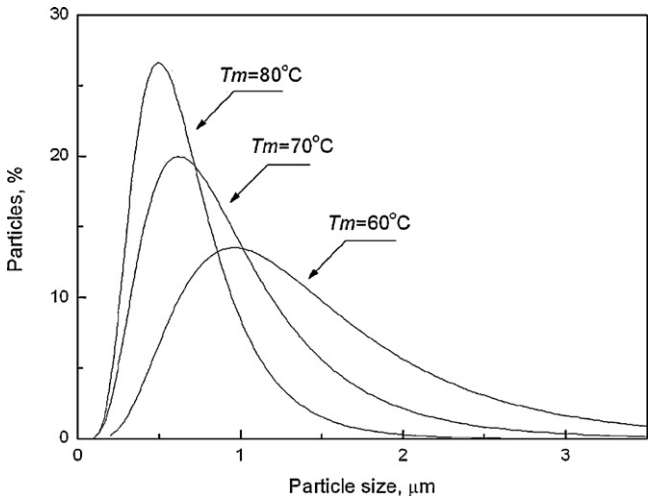

Fig. 3. Particle size distributions of micronized NaCS at different mixer temperature *Tm* with the solution concentration of 2.4 mg ml^{-1} in terms of particle number.

the particles cohered together. Some particles occupied the concavity on their surfaces with the large size nearly 5 μm. When the mixer pressure was increased to 10.0 MPa, the most remarkable change was that the NaCS microparticles were well-separated with a perfect spherical morphology and uniform particle size distribution between 0.2 and 4.5 μm. As shown in Fig. 4, obviously the size of these particles moved to a smaller diameter and narrower distribution with the increase of the mixer pressure. The particles prepared under the 11.5 MPa were also well-defined spherical state with narrowest PSD between 0.3 and 3.5 μm.

In theory, the SAA is a complex process involving thermodynamics, hydrodynamics, mass transfer, atomization, secondary atomization and precipitation kinetics [12–16]. It was based on the improvement of the mixing efficiency and the atomization status that the approach of the mixer pressure affecting the particle morphologies and size distributions. According to the VLE data of binary system of water–CO_2, the quantities of CO_2 in the aqueous solution increased slightly with the increase of the mixer pressure without considering the presence of the solute; however, it is elucidated that the interfacial tension of water/CO_2 reduced from 30 mN m^{-1} at 6.0 MPa to 20 mN m^{-1} at 8.0 MPa at a temperature of 40 °C after the near-equilibrium formed [20]. Consequently, the higher pressure can make the primary droplets more homogeneous and cause more drastic primary and secondary atomization [12], which resulted in the production of smaller particles with narrower size distribution. In this experiment, the pressure of 11.5 MPa should be considered as the suitable mixing pressure to prepare the smaller microspheres with smooth surface and narrow distribution adapted to the pharmaceutical engineering.

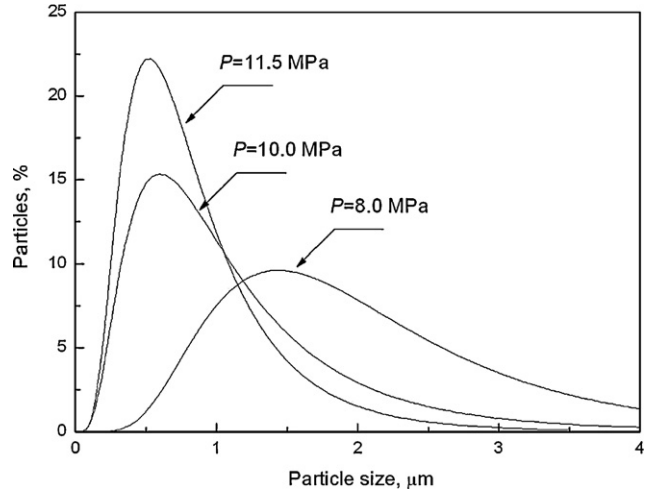

Fig. 4. Particle size distributions of micronized NaCS at different mixer pressure *P* with the solution concentration of 5.0 mg ml^{-1} in terms of particle number.

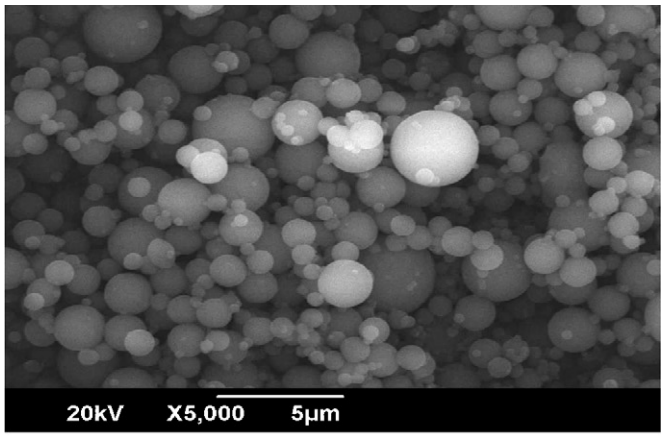

(a) ×5000

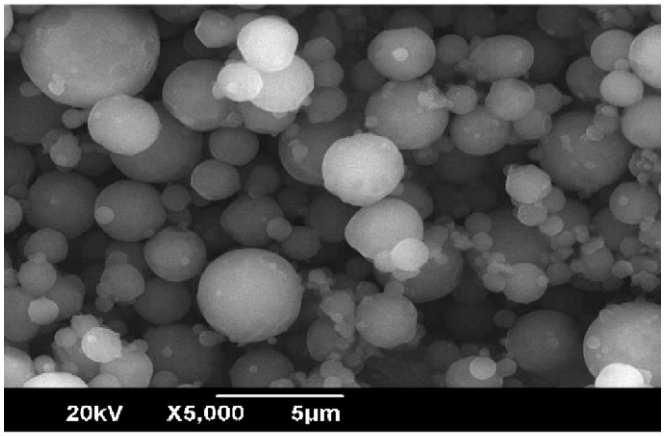

(b) ×5000

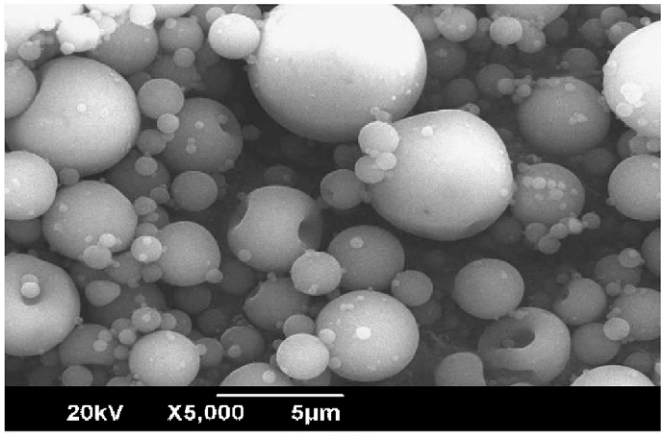

(c) ×5000

Fig. 5. SEM micrographs of NaCS precipitated by SAA-HCM from runs 7 to 9 with different mass flow ratio, at (a) *R* = 2.0, (b) *R* = 1.5, and (c) *R* = 0.7, *Tm* = 70 °C, *P* = 9.0 MPa, *Tp* = 100 °C, *C* = 2.4 mg ml^{-1}, and *Mw* = 633 kDa.

3.3. Effect of the mass flow ratio

The influence of the mass flow ratio R between the CO_2 and liquid solution on SAA-HCM processed NaCS particles can be qualitatively evaluated from Fig. 5 in the experimental conditions 7–9, where SEM micrographs of processed material at various R were reported. It can be seen that most particles were smaller than 5.0 μm with well-defined spherical morphology and smooth surface at $R = 2.0$ or 1.5. The PSDs of different mass flow ratio R in terms of particle number are given in Fig. 6. The mode of these distributions moved to smaller diameters and the PSD became narrower with the increasing R.

Undoubtedly, the operating points in this work always fell into a vapor–liquid coexistence region using water as a solvent. The antisolvent effect of the SC-CO_2 could be ignored and the effect of the mass flow ratio on the solubility of the CO_2 in the liquid was also negligible. However, with the decrease of the mass flow ratio R, the mass flow rate of the liquid solution increased, which led to the increase of the liquid film thickness [27]. When the amount of the SC-CO_2 was reduced to certain degree, the droplets formed with larger size because of the weak atomization and the final precipitates became larger and non-uniform. In addition, the phenomenon of the blocking in the nozzle and the lack of heat supply in precipitator may result in the inconvenience of the whole operation. In this section, $R = 2.0$ was the suitable process condition for the preparation of the NaCS microspheres.

3.4. Effect of the precipitator temperature

In the precipitator, a two-step atomization is obtained: the primary droplets produced at the outlet of the injector (pneumatic atomization) are further divided into secondary droplets by CO_2 expansion from the inside of the primary ones (decompressive atomization) [12]. The evaporation of the primary and secondary droplets in the precipitator can be established as a coupled heat and mass transport process. The optimization of the precipitator temperature is helpful to understand the particle formation mechanism and improve the morphology of the microparticles. This experiment was initiated at a lower precipitator temperature to avoid particles sintering or degradation. As shown in Fig. 7(a), collapsed and coalescing particles, which can be attributed to a partial recondensation of the solvent on the precipitates, or even an inefficient evaporation of the droplets caused by low precipitator temperature of 80 °C, were obtained. When the precipitator temperature was increased up to 100 °C, the well-defined spherical dried particles were collected as discussed in the previous section. In addition, most of the particles were formed as deflated balloons. It indicates that the particles were possibly hollow with the increase of the precipitator temperature from 100 to 120 °C in Fig. 7(b). The appearance of the toroidal particles was possible due to the hydrodynamic effect and the loss of structural stability of a droplet in a two-phase flow field [28].

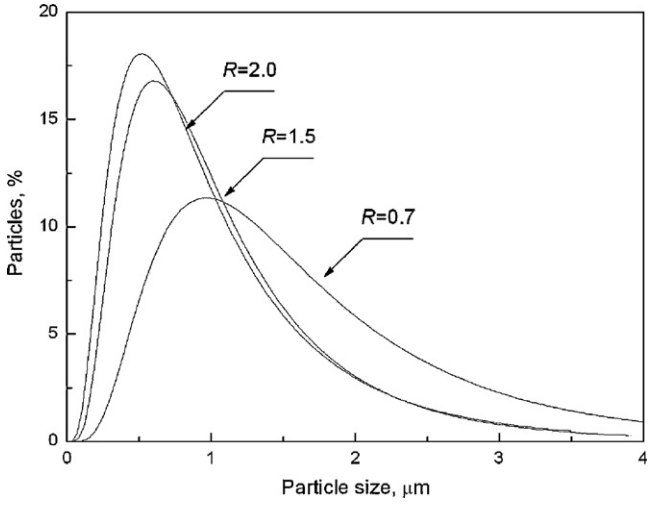

Fig. 6. Particle size distributions of micronized NaCS at different mass flow ratio R with the solution concentration of 2.4 mg ml^{-1} in terms of particle number.

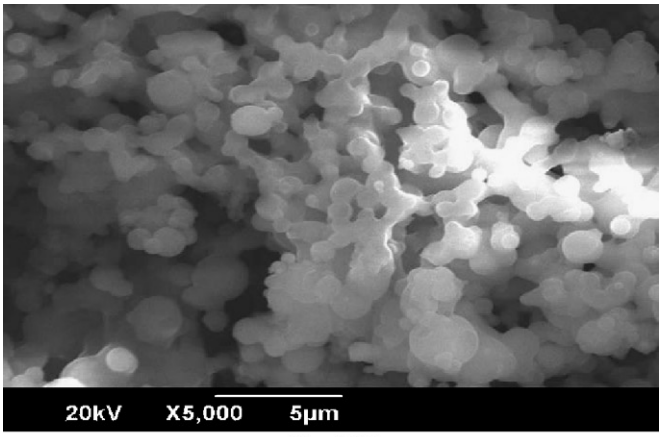

(a) ×5000

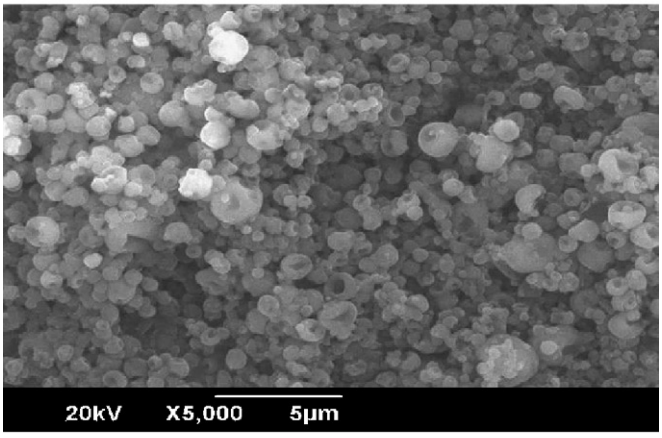

(b) ×5000

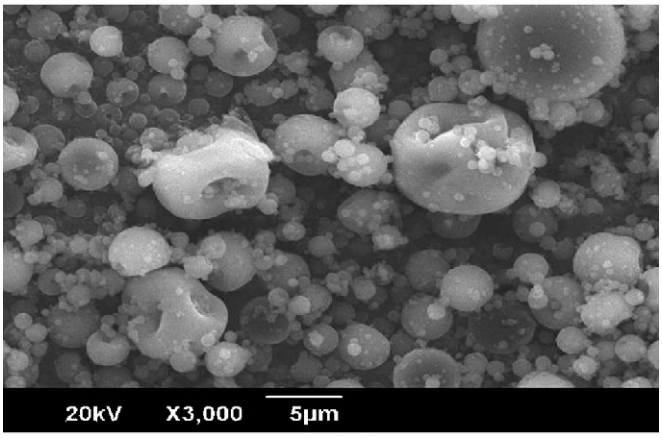

(c) ×5000

Fig. 7. SEM micrographs of NaCS precipitated by SAA-HCM from runs 10 to 12 with different precipitator temperature, (a) $Tp = 80$ °C, (b) $Tp = 120$ °C, water as the solvent, $C = 1.0$ mg ml^{-1}, and (c) $Tp = 100$ °C, water and ethanol (2:1) as the cosolvent, $C = 12.0$ mg ml^{-1}, the other parameters set at $R = 2.0$, $Tm = 70$ °C, and $Mw = 633$ kDa.

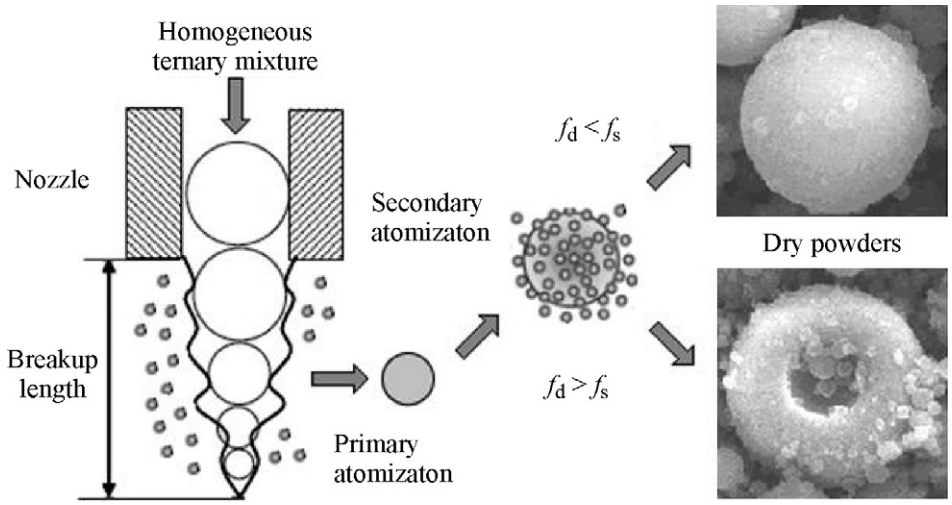

Fig. 8. The mechanism of the particle morphology development during dry process in the precipitator of the SAA-HCM process (f_d: the drag force; f_s: the surface tension).

Fig. 8 shows the mechanism of the transformation on the particle morphology during the dry process. According to the "one-droplet-one-particle" mechanism, a two-step atomization was performed: the primary pneumatic atomization and the secondary decompressive atomization. During the secondary atomization process, the velocity difference between the vapor and liquid phase resulted in the drag force. This force went against with the restoring force supplied by the surface tension. If the drag force was larger than the restoring force, the distortion would present on the surface of the secondary droplets. Due to the increase of the solute concentration during the subsequent dry process, the ability of restoring the spherical shape became weaker. Finally, the particles were formed by deflated balloons. It was also proved in Fig. 5. When the mass flow ratio *R* decreased to 0.7, there were several concavities on the surface of the powder. The reason is that with the decrease of *R*, the mass flow rate of the liquid mixture increases and thus leads to the increase of thickness of the liquid film. Therefore, the droplets formed by the SAA-HCM process became large resulted in the reduction of the droplets' structural stability. Similarly, when a measured amount of ethanol was added to the solution in the run 12, it acted as the surfactant to change the interfacial forces in the SC-CO_2–water system [29]. Besides, the evaporation of the ethanol was faster than that of water as a solvent. Consequently, the stability of the droplets decreased and the morphology of prepared particles showed an unstable shape in Fig. 7(c). In this section, 100 °C was chosen as the suitable precipitator temperature, since it can make solvent volatilize completely without any change of the particles morphology.

3.5. Effect of the liquid solution concentration

The influence of the liquid solution concentration *C* on SAA-HCM processed NaCS particles were investigated in the series of runs 13–16. When the solute concentration *C* was confined at 1.0 mg ml^{-1}, the particles treated successfully by SAA-HCM were quite small with a very sharp PSD between 0.1 and 1.5 μm and a noncoalescing spherical morphology. From the quantitative measurement of PSDs in terms of particle number in Fig. 9, it is obvious that the particle size became larger and the PSD became wider with the increase of the solution concentration. While the solution concentration was set at 12.0 mg ml^{-1}, the particle size distribution of precipitates ranged from 0.4 to 6.0 μm.

The viscosity and the surface tension of the ternary mixture were enhanced notably with the increase of the solution concentration. Hence, the insufficient atomization resulted in the formation of larger primary droplets, insufficient subsequent atomization and the non-uniform particles. By adjusting these parameters properly, SAA-HCM was considered as one of the most promising micronization methods which can prepare the microparticles with perfect surface and controlled particle size distribution in a desired range. In this part, the solution concentration of 2.0 mg ml^{-1} is suitable for the preparation of the NaCS particles with PSD between 0.3 and 3.0 μm.

3.6. Effect of the molecular weight of NaCS

The morphology and size of the precipitated particles were not only influenced by the process parameters in the SCF-based atomization, but also dependent upon the physicochemical properties of the material to be treated. It has been reported that various species of the particles morphology, such as spherical [16], needle-like [9], crystal [9], doughnut-like [15], *etc.*, presented in different substances micronization under the similar process conditions. Hence, it is necessary to get a correlation between the physicochemical properties of the polymer and the state of the precipitates. One of the most significant properties of the NaCS is the substitution degree (*DS*) of the sulfate group [22], which depicted the number of sulfate groups at every glucose ring. The higher the *DS* of

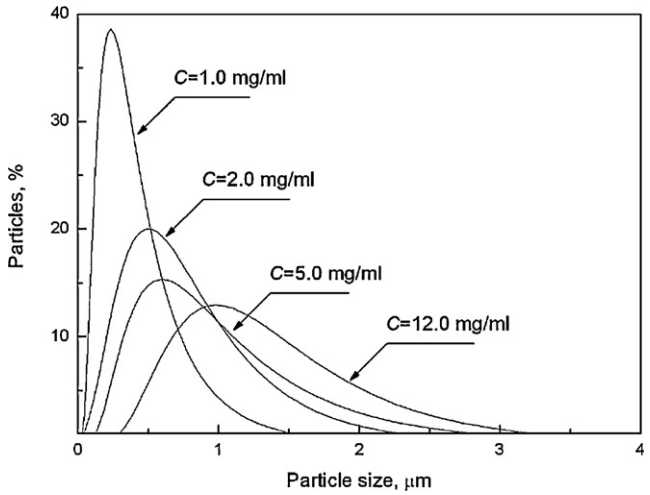

Fig. 9. Particle size distributions of micronized NaCS at different solute concentration *C* in terms of particle number.

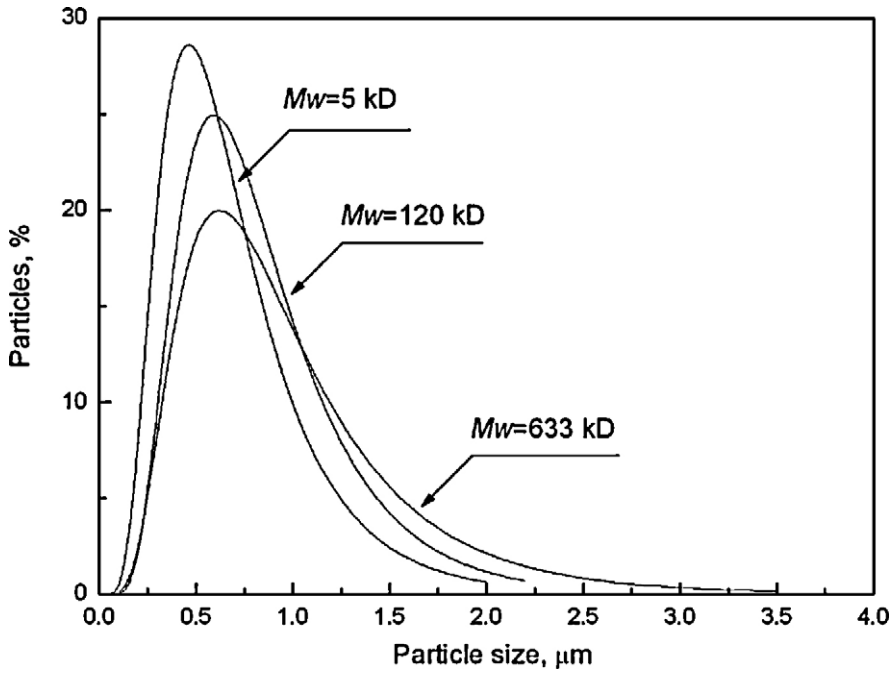

Fig. 10. Particle size distributions of micronized NaCS at different molecular weight *Mw* with the solute concentration of 2.4 mg ml^{-1} in terms of particle number.

the NaCS polymer, the shorter sulfated cellulose chains with lower molecular weight *Mw* and higher polarity will get. Different molecular weights of NaCS polymer, obtained by controlling the DS of the sulfate groups, were micronized by SAA-HCM process in runs 17–19. Fig. 10 shows the particle size distribution curves measured at different *Mw* in the terms of particle number. When the *Mw* of NaCS was 633 kDa, well-defined spherical microparticles were prepared with the size distribution between 0.5 and 3.5 μm. With the decrease of the molecular weight, basically no change occurred on the morphology of the particles with spherical shape; however, the particle size distribution curves tended to be sharper and moved towards small diameter region. In the run 19, a very sharp PSD between 0.3 and 2.0 μm were obtained when the *Mw* of NaCS was set at 5 kDa.

With the increase of the molecular weight, the soluble rate of the NaCS polymer reduced, hence the viscosity and the surface tension of the corresponding solution increased obviously. These factors will result in the insufficient mixing and atomization which is in favor of the formation of larger microparticles. Otherwise, when the viscosity is increased to a certain value, the blocking of the nozzle will result in the discontinuity and unsuccessful micronization. Consequently, the *Mw* should be chosen carefully in order to satisfy the request of the successful polymer micronization process and the drug delivery system.

3.7. FITR characterization

Fig. 11 shows the FTIR spectra of untreated NaCS and SAA-HCM processed NaCS with the *Mw* of 633 kDa and 120 kDa, respectively. The representative bands for sodium cellulose sulfate could be summarized as follows: the broad absorption at 3419–3440 cm^{-1} related to the stretching of H-bonded OH groups, and those at 2895–2921 cm^{-1} to C–H stretching [30–32]. The absorption peak at 1641–1644 cm^{-1} appeared in cellulose main structure itself and did not vary in intensity in the sulfation process [33]. The strong peaks at 1065–1073 cm^{-1} were indicative of C–O stretching at C-3, C–C stretching and C–O stretching at C-6 [34,35]. As the derivative of cellulose, NaCS showed the following characteristic peaks: as a sulfate it showed strong absorption bands of S=O at 1233–1260 cm^{-1} and C–O–S at 811–817 cm^{-1}. These main absorption bands all presented similarly in Fig. 11(a)–(d), which demonstrated that no significant change occurred in the NaCS main structure after SAA-HCM processed. With the increase of the substitution degree, the absorption bands of S=O and C–O–S became much stronger because of the enhancement of the sulfate group. Hence, it is proven that the SAA-HCM process has no effect on NaCS main structure.

3.8. XRD characterization

Since drying can also affect the NaCS morphology, X-ray analysis was preformed on the untreated and SAA-HCM processed NaCS to evaluate the effect of the SAA-HCM process on the solid state of the polymer. In the literature [36], NaCS is an amorphous polysaccharide in the dry state and the main chain motion of NaCS is not observed due to strong intermolecular interaction. The

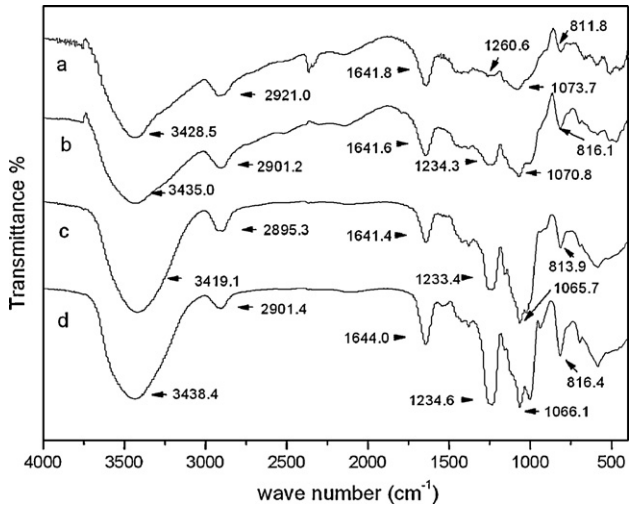

Fig. 11. The FTIR analysis of the untreated NaCS material (a) *Mw* = 633 kDa, (b) *Mw* = 120 kDa and the NaCS microparticles (c) *Mw* = 633 kDa, (d) *Mw* = 120 kDa prepared by SAA-HCM.

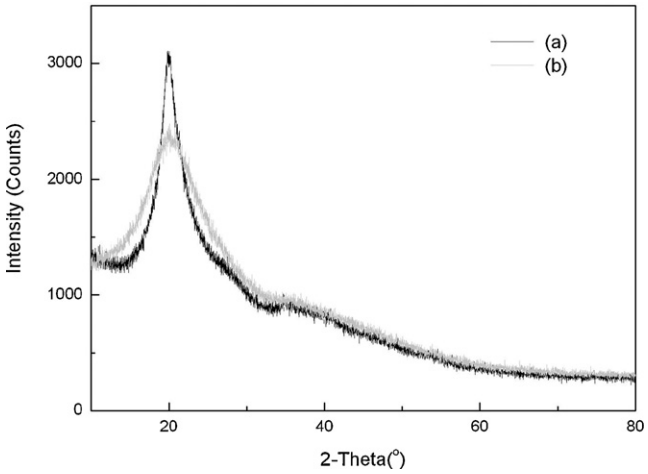

Fig. 12. The XRD analyses of (a) the unprocessed NaCS material and (b) the NaCS microparticles prepared by SAA-HCM with the molecular weight of 633 kDa.

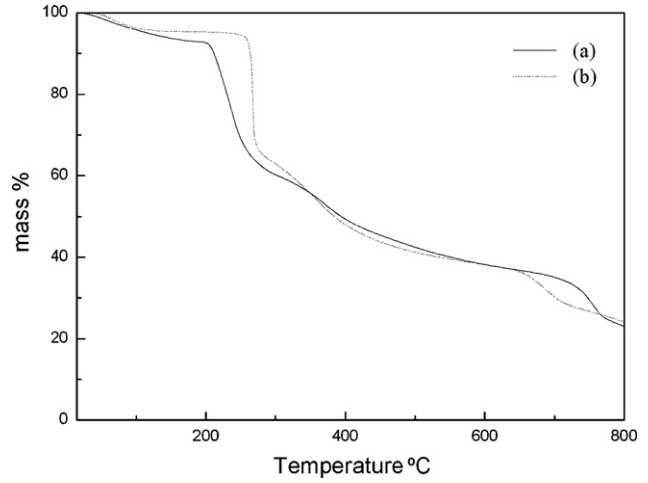

Fig. 13. The TGA analyses of (a) the unprocessed NaCS material and (b) the NaCS microparticles prepared by SAA-HCM with the molecular weight of 633 kDa.

XRD-analysis results, reported in Fig. 12, both unprocessed NaCS material and the NaCS precipitates after SAA-HCM processing were completely amorphous.

3.9. TGA characterization

The NaCS material showed no phase transition until the thermal decomposition occurred by differential scanning calorimetry because of the amorphous state. Therefore, the thermal properties of the NaCS microparticles and the untreated NaCS material were investigated by the thermo-gravimetric analysis (TGA) showed in Fig. 13. After initial loss of moisture and desorption of gases at about 30–202 °C, a major decomposition proceeded from 202 to 259 °C for untreated NaCS. For modified NaCS by SAA-HCM, there was a major decomposition initiated at 252 °C. That meant the thermal stability of the NaCS material was enhanced by SAA-HCM treated because NaCS was pre-disposed by heated to 100 °C.

4. Conclusions

The hydrophilic biodegradable polymer NaCS was successfully micronized to well-defined spherical microparticles *via* the novel process of SAA-HCM with pure water as the sole solvent. The influences of the process parameters on particle size and particle size distributions were investigated. It was found that using higher mixer pressure *P* and the lower solute concentration *C* were favorable to reduce the average size of the resultant precipitates. As also evidenced from the experimental results, the molecular weight *Mw* of the NaCS should be one of the crucial factors to control the uniformity of the particulates. When the molecular weight *Mw* was set at 5 kDa, the uniform microspheres with narrow PSD (0.3–2.0 μm) and perfect spherical morphology were obtained. High precipitator temperature *Tp* could make the presence of the deflated balloons in the precipitates. This transformation of the spherical droplet was caused by the hydrodynamic effect and the loss of structural stability of the droplet in a two-phase flow field. Compared with unprocessed material, there was no significant change on the main structure and the stability of the NaCS powders prepared by SAA-HCM as shown by the FTIR spectra. The XRD patterns revealed that both the unprocessed NaCS and the samples after SAA-HCM processing were completely amorphous. Besides, the results from TGA analysis indicated that the thermal stability of the NaCS was enhanced after processed by this technique. In summary, the successful micronization of NaCS allowed the extension of SAA-HCM applications to the hydrophilic material. In addition, these results manifested the potentials of producing protein pharmaceutical NaCS composites with controlled size distributions for sustained-release in various drug delivery strategies using this supercritical fluid process without any organic solvent residual.

Acknowledgement

The authors thank gratefully for the financial support provided by the National Natural Science Foundation of China (No. 20676118, No. 20876139).

References

[1] Y. Yang, N. Bajaj, P. Xu, K. Ohn, M.D. Tsifanskym, Y. Yeo, Development of highly porous large PLGA microparticles for pulmonary drug delivery, Biomaterials 30 (2009) 1947–1953.
[2] S.D. Yeo, E. Kiran, Formation of polymer particles with supercritical fluids: a review, J. Supercrit. Fluids 34 (2005) 287–308.
[3] D.A. Edwards, J. Hanes, G. Caponetti, J. Hrkach, A.B. Jebria, M.L. Eskew, J. Mintzes, D. Deaver, N. Lotan, R. Langer, Large porous particles for pulmonary drug delivery, Science 276 (1997) 1868–1872.
[4] L.H. Mei, S.J. Yao, Cultivation and modeling of encapsulated *Saccharomyces cerevisiae* in NaCS–PDMDAAC polyelectrolyte complexes, J. Microencapsul. 19 (4) (2002) 397–405.
[5] X.C. Fu, G.P. Wang, W.Q. Liang, M.S.S. Chow, Prediction of drug release from HPMC matrices: effect of physicochemical properties of drug and polymer concentration, J. Control. Release 95 (2004) 209–216.
[6] R.C. Petersen, D.W. Matson, R.D. Smith, The formation of polymer fibers from the rapid expansion of supercritical fluid solutions, Polym. Eng. Sci. 27 (2004) 1693–1697.
[7] E. Reverchon, G.D. Porta, I.D. Rosa, P. Subra, D. Letourneur, Supercritical antisolvent micronization of some biopolymers, J. Supercrit. Fluids 18 (2000) 239–245.
[8] J. Kerc, S. Srcic, Z. Knez, P. Sencar-Bozic, Micronization of drugs using supercritical carbon dioxide, Int. J. Pharm. 182 (1993) 33–39.
[9] E. Reverchon, Supercritical assisted atomization to produce micro and/or nanoparticles of controlled size and distribution, Ind. Eng. Chem. Res. 41 (10) (2002) 2405–2411.
[10] E. Reverchon, Process for production of micro and/or nano particles, WO Patent 03/004142 (2003).
[11] E. Reverchon, G.D. Porta, Particle design using supercritical fluids, Chem. Eng. Technol. 26 (2003) 840–845.
[12] E. Reverchon, A. Antonacci, Chitosan microparticles production by supercritical fluid processing, Ind. Eng. Chem. Res. 45 (16) (2006) 5722–5728.
[13] E. Reverchon, G. Lamberti, A. Antonacci, Supercritical fluid assisted production of HPMC composite microparticles, J. Supercrit. Fluids 46 (2008) 185–196.
[14] E. Reverchon, A. Antonacci, Drug–polymer microparticles produced by supercritical assisted atomization, Biotechnol. Bioeng. 97 (6) (2007) 1626–1637.
[15] E. Reverchon, G.D. Porta, Micronization of antibiotics by supercritical assisted atomization, J. Supercrit. Fluids 26 (2003) 243–252.
[16] E. Reverchon, G.D. Porta, Terbutaline microparticles suitable for aerosol delivery produced by supercritical assisted atomization, Int. J. Pharm. 258 (2003) 1–9.

[17] M.Q. Cai, Y.X. Guan, S.J. Yao, Z.Q. Zhu, Supercritical fluid assisted atomization introduced by hydrodynamic cavitation mixer (SAA-HCM) for micronization of levofloxacin hydrochloride, J. Supercrit. Fluids 43 (2008) 524–534.
[18] A. Pal, A. Verma, S.S. Kachhwaha, S. Maji, Biodiesel production through hydrodynamic cavitation and performance testing, Renew. Energy 35 (2010) 619–624.
[19] J.B. Ji, J.L. Wang, Y.C. Li, Y.L. Yu, Z.C. Xu, Preparation of biodiesel with the help of ultrasonic and hydrodynamic cavitation, Ultrasonics 44 (2006) e411–e414.
[20] T. Frederic, B. Frank, Thermodynamic and dynamic interfacial properties of binary carbon dioxide–water systems, J. Phys. Chem. B 108 (2004) 2405–2412.
[21] J. Mansfeld, M. Förster, A. Schellenberger, H. Dautzenberg, Immobilization of invertase by encapsulation in polyelectrolyte complexes, Enzyme Microb. Technol. 13 (1991) 240–244.
[22] S.J. Yao, An improved process for the preparation of sodium cellulose sulphate, J. Chem. Eng. 78 (2000) 199–204.
[23] Y.L. Xie, M.J. Wang, S.J. Yao, Preparation and characterization of biocompatible microcapsules of sodium cellulose sulfate/chitosan by means of layer-by-layer self-assembly, Langmuir 25 (16) (2009) 8999–9005.
[24] V. Stadlbauer, P.B. Stiegler, S. Schaffellner, O. Hauser, G. Halwachs, F. lberer, K.H. Tscheliessnigg, C. Lackner, Morphological and functional characterization of a pancreatic β-cell line microencapsulated in sodium cellulose sulfate/poly (diallyldimethylammonium chloride), Xenotransplantation 13 (2006) 337–344.
[25] M.J. Wang, Y.L. Xie, Q.D. Zheng, S.J. Yao, A novel potential microflora-activated carrier for a colon-specific drug delivery system and its characteristics, Ind. Eng. Chem. Res. 48 (11) (2009) 5276–5284.
[26] A. Bamberger, G. Sieder, G. Maurer, High-pressure (vapor + liquid) equilibrium in binary mixtures of (carbon dioxide + water or acetic acid) at temperatures from 313 to 353 K, J. Supercrit. Fluids 17 (2000) 97–110.
[27] M.C. Zhang, Y. Lu, J.Y. Wang, H.J. fan, D.G. Li, Q.F. Chen, Mathematical modeling on the gas–liquid two phase flow in the Y-jet nozzle and its atomization process, J. Combus. Sci. Technol. 6 (3) (2000) 205–209.
[28] F. Iskandar, L. Gradon, K. Okuyama, Control of the morphology of nanostructured particles prepared by the spray drying of a nanoparticle sol, J. Colloid Interface Sci. 265 (2003) 296–303.
[29] Z.Y. Li, J.Z. Jiang, X.W. Liu, H.H. Tang, W. Wei, Experimental investigation on the micronization of aqueous cefadroxil by supercritical fluid technology, J. Supercrit. Fluids 48 (2009) 247–252.
[30] Y. Cao, H. Tan, Structural characterization of cellulose with enzymatic treatment, J. Mol. Struct. 705 (2004) 185–193.
[31] L.L. Wang, G.T. Han, Y.M. Zhang, Comparative study of composition, structure and properties of *Apocynum venetum* fibers under different pretreatments, Carbohydr. Polym. 69 (2007) 391–397.
[32] K.K. Pandey, Study of the effect of photo-irradiation on the surface chemistry of wood, Polym. Degrad. Stab. 90 (2005) 9–20.
[33] C.Y. Yin, J.B. Li, Q. Xu, Q. Peng, Y.B. Liu, X.Y. Shen, Chemical modification of cotton cellulose in supercritical carbon dioxide: synthesis and characterization of cellulose carbamate, Carbohydr. Polym. 67 (2007) 147–154.
[34] S.Y. Oh, D.I. Yoo, Y. Shin, H.C. Kim, H.Y. Kim, Y.S. Chung, W.H. Park, J.H. Youk, Crystalline structure analysis of cellulose treated with sodium hydroxide and carbon dioxide by means of X-ray diffraction and FTIR spectroscopy, Carbohydr. Res. 340 (2005) 2376–2391.
[35] C.F. Liu, F. Xu, J.L. Ren, S. Curling, R.C. Sun, P. Fowler, M.S. Baird, Physicochemical characterization of cellulose from perennial ryegrass leaves (*Lolium perenne*), Carbohydr. Res. 341 (2006) 2677–2687.
[36] T. Hatakeyama, H. Yoshida, H. Hatakeyama, The liquid crystalline state of water–sodium cellulose sulphate systems studied by DSC and WAXS, Thermochim. Acta 266 (1995) 343–354.